

Intelligent fuzzy inference system approach for modeling of debonding strength in FRP retrofitted masonry elements

Mohsen Khatibinia^{*1} and Mohammad Reza Mohammadizadeh^{2a}

¹Department of Civil Engineering, University of Birjand, Birjand, Iran

²Department of Civil Engineering, Hormozgan University, Bandar Abbas, Iran

(Received July 17, 2016, Revised November 17, 2016, Accepted November 17, 2016)

Abstract. The main contribution of the present paper is to propose an intelligent fuzzy inference system approach for modeling the debonding strength of masonry elements retrofitted with Fiber Reinforced Polymer (FRP). To achieve this, the hybrid of meta-heuristic optimization methods and adaptive-network-based fuzzy inference system (ANFIS) is implemented. In this study, particle swarm optimization with passive congregation (PSOPC) and real coded genetic algorithm (RCGA) are used to determine the best parameters of ANFIS from which better bond strength models in terms of modeling accuracy can be generated. To evaluate the accuracy of the proposed PSOPC-ANFIS and RCGA-ANFIS approaches, the numerical results are compared based on a database from laboratory testing results of 109 sub-assemblages. The statistical evaluation results demonstrate that PSOPC-ANFIS in comparison with ANFIS-RCGA considerably enhances the accuracy of the ANFIS approach. Furthermore, the comparison between the proposed approaches and other soft computing methods indicate that the approaches can effectively predict the debonding strength and that their modeling results outperform those based on the other methods.

Keywords: debonding strength; Fiber Reinforced Polymer; adaptive-network-based fuzzy inference system; particle swarm optimization; real coded genetic algorithm

1. Introduction

In recent years, more attention has been devoted to the development of innovative materials and advanced technologies applied in the preservation of cultural heritage buildings. Fiber Reinforced Polymer (FRP) has been utilized as a strengthening solution and successfully employed for retrofitting masonry buildings and existing structures (Mohammadizadeh and Fadaee 2009, Mohammadizadeh *et al.* 2009, Mohammadizadeh and Fadaee 2010, Abdollahi Chahkand *et al.* 2014). Advantages of FRP include the low specific weight, corrosion immunity and high tensile strength. In the past decade, the characterization of FRP strengthened concrete structures has been considered as a top priority in civil engineering. Furthermore, a number of researches have dealt with masonry buildings, particularly ancient ones due to especially important ancient buildings (Ceroni *et al.* 2014). For masonry buildings, structural performance can be improved using externally bonded FRP retrofits that represent an effective, cost-effective and acceptable approach.

The performance and efficiency of externally bonded strengthening procedures depend largely on the capability of the FRP-masonry interface to provide an efficient

mechanism for transferring loads (Oliveira *et al.* 2010). Bond loss in FRP reinforcement, i.e., the debonding failure, usually leads to failure. In FRP strengthened masonry elements common out-of plane failure mechanisms include sliding of masonry units, flexural-shear cracking, FRP rupture, FRP debonding, punching shear and crushing of brick in compression (Kashyap *et al.* 2012, Ceroni *et al.* 2014). The strength and ductility of a masonry member retrofitted with longitudinal externally bonded FRP are mostly influenced by the intermediate crack debonding failure mechanism (Kashyap *et al.* 2012). The mechanism of the bond is highly complicated due to the mechanical properties of masonry blocks, mortar joints, adhesive and FRP reinforcement (Ceroni *et al.* 2014). In recent years, numerous numerical and analytical studies have been conducted to determine and formulate the service and ultimate debonding limit states of FRP external reinforcements. In order to achieve this purpose, various experimental setups have been introduced. The results have provided parametric relations defining resistance against debonding as a function of the main parameters involved (Ceroni *et al.* 2014, Carrara and Freddi 2014). Furthermore, in practical applications this resistance can be estimated using soft computing, numerical and analytical methods.

Soft computing techniques have been introduced as the modern approach for constructing a computationally intelligent system. The main aim of the techniques is to emulate human mind as closely as possible (Jang *et al.* 1996). The most popular of the techniques consists of Artificial Neural Networks (ANNs), Evolutionary Computation (EC), Machine Learning (ML), Fuzzy Logic

*Corresponding author, Assistant Professor

E-mail: m.khatibinia@birjand.ac.ir

^aAssistant Professor

(FL) and support vector machines. The successful applications of the techniques have been reported in the problems of engineering (Gholizadeh and Salajegheh 2009, Seyedpoor *et al.* 2009, Gholizadeh *et al.* 2009, Helmy *et al.* 2011, Khatibinia *et al.* 2013, Khatibinia *et al.* 2013, Khatibinia and Khosravi 2014, Gharehbaghi and Khatibinia 2015, Tsai *et al.* 2015, Yuksel and Yazar 2015, Gholizadeh 2015, Khatibinia *et al.* 2015, Chitti *et al.* 2016, Khatibinia *et al.* 2016). The ANN techniques were proposed to predict the shear strength of FRP-reinforced concrete flexural members without stirrups (Lee and Lee 2014). The compressive strength of light weight concrete was successfully modeled using regression, ANN and adaptive neuro fuzzy inference system (ANFIS) (Sadrmomtazi *et al.* 2013). Ozan *et al.* (2009) investigated the accuracy of ANN and fuzzy logic models in order to estimate the long-term compressive strength of silica fume concrete. Golafshani *et al.* (2012) predicted the bond strength of spliced steel bars in concrete using ANN and fuzzy logic. Compressive strength for different concrete types has also been predicted using ANNs and ANFIS (Alshihri *et al.* 2009, Sobhani *et al.* 2010, Słonski 2010, Jalal and Ramezaniapour 2012). Bal and Buyle-Bodin (2013) proposed ANN to accurately predict the dimensional variations due to drying shrinkage of concrete. Perera *et al.* (2014) predicted the performance of RC beams shear strengthened with near-surface mounted FRP rods using ANN. In this work, a multi-objective optimization problem was solved to generate a design formula for easy application and to find the shear strength contribution supplied through a near-surface mounted system. Plevris and Asteris (2014) used ANN to provide an approximation for the failure surface in masonry materials. In the work of Bedirhanoglu (2014), the neuro-fuzzy (NF) technique was investigated for estimating modulus of elasticity of concrete. Also, in this study a new simple NF model by implementing a different NF system approach was proposed. Recently, Mansouri and Kisi (2015) have compared the accuracy of ANFIS with that of ANN for prediction of debonding strength for masonry elements retrofitted with FRP composites.

This study proposes an intelligent ANFIS approach in order to predict debonding strength of masonry elements retrofitted with FRP. To achieve this purpose, particle swarm optimization with passive congregation (PSOPC) and real coded genetic algorithm (RCGA) as metaheuristic techniques are utilized to find the best parameters of the ANFIS model from which better bond strength models in terms of modeling accuracy can be generated. In this proposed method, the subtractive algorithm (SA) (Chiu 1994) is utilized to find the optimum number of fuzzy rules. Furthermore, the fuzzy c-means (FCM) approach (Bezdek 1981) creates a fuzzy inference system in the simulation of the ANFIS model. The effectiveness and accuracy of the proposed PSOPC-ANFIS and RCGA-ANFIS are investigated based on modeling results of a laboratory database form 109 sub-assemblages in two stages. At first, the statistical evaluation results of PSOPC-ANFIS and RCGA-ANFIS reveal that the PSOPC-ANFIS model in comparison with the RCGA-ANFIS model considerably enhances the accuracy of ANFIS, the optimal solution and

the coverage rate. In second stage, the prediction results of PSOPC-ANFIS and RCGA-ANFIS are compared with those obtained based on the original ANFIS, ANN and multiple nonlinear regression (MNL) approaches. The comparison results indicate that the proposed PSOPC-ANFIS and RCGA-ANFIS are more accurate than ANFIS, ANN and MNL approaches.

2. Existing shear bond strength model of FRP

Failure in masonry elements externally bonded with FRP is usually accompanied by debonding of reinforcement due to shear stress. The shear behavior of reinforcement bonded to the support and under a force parallel to the bond surface can be modeled based on the shear stress-tangential slip law (Ceroni *et al.* 2014) which par excellence can occur in conjunction with a normal stress-displacement law (Pan and Leung 2007, De Lorenzis *et al.* 2010). Thus, the maximum transmissible force is related to the mechanical characteristics of the support. This can be also evaluated using cohesive fracture mechanics methods. In the case of masonry, this is largely dependent upon the elements making the masonry itself, i.e., the tensile strength of masonry bricks and mortar. In general, for FRP bonded on supports consisting of brittle materials and infinite anchorage length, the maximum transmissible load is given by

$$P_{\max} = -b_f \int_0^{\infty} \tau(x) dx \quad (1)$$

where b_f represents the reinforcement width, x is the longitudinal axis and $\tau(x)$ is the bond shear stress distribution along the interface.

The fracture energy related to the area below the interface bond shear stress-slip law (see Fig. 1) corresponds to the energy needed to bring a local bond element to full shear fracture. The fracture energy is given as following

$$G_c = -b_f \int_0^{\infty} \tau(s) ds \quad (2)$$

In the case of a bond-slip model based on an interface bond shear stress-slip law $\tau(x)$, the following relation holds between the maximum transmissible force P_{\max} (i.e., debonding load) and the fracture energy (G_c) of the interface law (Ferracuti *et al.* 2006, De Lorenzis *et al.* 2010)

$$P_{\max} = b_f \sqrt{2E_p t_p G_c} \quad (3)$$

where E_p and t_p represent elastic modulus and thickness of FRP, respectively. The fracture energy is expressed as follows

$$G_c = K_b K_G \sqrt{f_c f_{ut}} \quad (4)$$

where K_b is a width factor coefficient for the effect of the reinforcement width on P_{\max} , K_G is a parameter to be calibrated through experimentation in bond tests, f_c is the compressive strength and f_{ut} is the tensile strength of the brittle support.

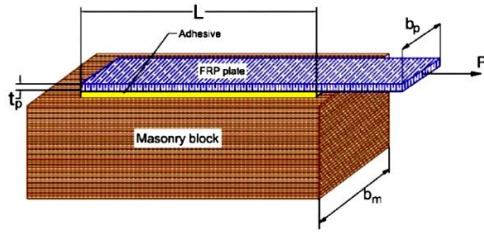


Fig. 1 Geometry of a masonry element retrofitted with FRP (Mansouri and Kisi 2015)

Numerous models have been introduced for the bond strength between FRP and concrete. Some of these models consist of parameters which is not applicable for masonry while for others sufficient information were not available to incorporate the models in the analysis (Kashyap *et al.* 2012). A number of bond strength models proposed for masonry were presented in the study implemented by Mansouri and Kisi (2015).

3. Experimental database

In order to obtain a general model based on soft computing for reliable debonding resistance of FRP retrofitted masonry elements, a database of laboratory testing results for 109 sub-assemblages expressed in the wok of Mansouri and Kisi (2015) is selected. The database is shown in Table 1.

Table 1 Experimental database

Input	Unit	Min	Max	Mean	Variance
L_b	mm	50	420	186.136	12013.43
b_p	mm	6.35	50	28.832	151.573
t_p	mm	0.12	6.35	1.048	1.219
E_p	MPa	22300	230000	95655.05	5.19×10^9
b_m	mm	200	400	257.018	4050.981
f_{ut}	MPa	1.3	3.57	2.517	0.702
P_{max}	kN	2.850	84.500	18.345	4.53×10^8

The input variables are thickness of the FRP strip (t_p), width of the FRP strip (b_p), Young's modulus of the FRP (E_p), bonded length (L_b), tensile strength of the masonry block (f_{ut}), width of the masonry block (b_m) and the maximum debonding force (P_{max}).

4. The concept of ANFIS model

A fuzzy inference system (FIS) has been introduced as a nonlinear mapping from the input space to the output space (Jang *et al.* 1997). The mapping mechanism is based on the conversion of inputs from numerical domain to fuzzy domain with using the three functional components: a rule base, which contains a selection of fuzzy rules; a database, which defines the membership functions (MFs) used in the fuzzy rules and a reasoning mechanism, which performs the inference procedure upon the rules to derive an output. The

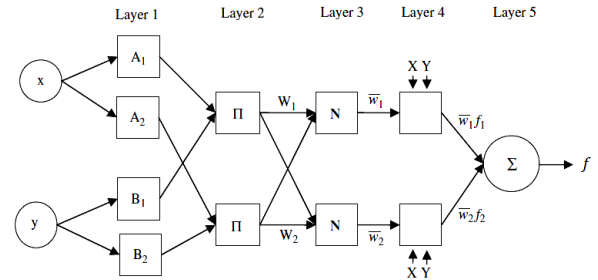


Fig. 2 The architecture of the ANFIS model

ANFIS approach is proposed a FIS implemented in the framework of adaptive networks (Jang *et al.* 1997). For simplicity a typical ANFIS shown in Fig. 2 consists of two fuzzy if-then rules based on Takagi and Sugeno's type (Jang *et al.* 1997)

$$\text{Rule 1: If } x \text{ is } A_1 \text{ and } y \text{ is } B_1, \text{ then } f_1 = p_1x + q_1y + r_1 \quad (5)$$

$$\text{Rule 2: If } x \text{ is } A_2 \text{ and } y \text{ is } B_2, \text{ then } f_2 = p_2x + q_2y + r_2$$

where A_1, A_2, B_1 and B_2 are labels for representing MFs for the inputs x and y , respectively. Also, p_i, q_i and r_i ($i=1,2$) are parameters of the output MFs (consequent parameters).

The general structure of ANFIS shown in Fig. 2 consists of fixed square nodes and adaptive circle nodes whose parameters are changed during the training process. A hybrid learning algorithm of ANFIS is employed by the parameters of MFs of input variables and linear parameters of the output variable. These parameters are optimized using gradient descent (GD) approaches. The final output of the given network with two inputs and one output in terms of the above parameters can be calculated as follows

$$f = \sum_i \bar{w}_i f_i = \frac{\sum_{i=1}^2 w_i f_i}{\sum_{i=1}^2 w_i}, \quad \text{for } i=1,2 \quad (6)$$

$$w_i = \mu A_i(x) \times \mu B_i(y) \quad \text{for } i=1,2 \quad (7)$$

where w_i is the firing strength of rule i , $\mu A_i(x)$ and $\mu B_i(y)$ are the membership degrees of x and y in A_i and B_i , respectively. Gaussian functions with maximum equal to 1 and minimum equal to 0 are selected for the membership degrees as

$$\mu A_i(x) = \frac{1}{1 + \left(\frac{x - c_i}{a_i}\right)^{2b_i}} \quad (8)$$

$$\mu B_i(y) = \frac{1}{1 + \left(\frac{y - d_i}{e_i}\right)^{2g_i}} \quad (9)$$

where $\{a_i, b_i, c_i\}$ and $\{d_i, e_i, g_i\}$ is the premise parameter set used to adjust the shape of MF.

5. Particle swarm optimization with passive congregation

Particle swarm optimization (PSO) algorithm is inspired by the social behavior of animals such as fish schooling,

insects swarming and birds flocking (Kennedy and Eberhart 2001). The PSO method was introduced by Kennedy and Eberhart (2001) to simulate the graceful motion of bird swarms as a part of a socio-cognitive study. It involves a number of particles that are initialized randomly in the search space of an objective function. The particles are referred to as swarm. Each particle of the swarm represents a potential solution of the optimization problem. The i th particle in t th iteration is associated with a position vector, \mathbf{X}_i^t , and a velocity vector, \mathbf{V}_i^t , as following

$$\begin{aligned}\mathbf{X}_i^t &= \{x_{i1}^t, x_{i2}^t, \dots, x_{iD}^t\} \\ \mathbf{V}_i^t &= \{v_{i1}^t, v_{i2}^t, \dots, v_{iD}^t\}\end{aligned}\quad (10)$$

where D is dimension of the solution space.

The particle fly through the solution space and its position is updated based on its velocity, the best position particle (***pbest***) and the global best position (***gbest***) that swarm has visited since the first iteration as

$$\mathbf{V}_i^{t+1} = \omega^t \mathbf{V}_i^t + c_1 r_1 (\mathbf{pbest}_i^t - \mathbf{X}_i^t) + c_2 r_2 (\mathbf{gbest}^t - \mathbf{X}_i^t) \quad (11)$$

$$\mathbf{X}_i^{t+1} = \mathbf{X}_i^t + \mathbf{V}_i^{t+1} \quad (12)$$

where r_1 and r_2 are two uniform random sequences generated from interval $[0, 1]$; c_1 and c_2 are the cognitive and social scaling parameters, respectively and ω is the inertia weight that controls the influence of the previous velocity. Shi and Eberhart (1998) proposed that the cognitive and social scaling parameters c_1 and c_2 should be selected as $c_1=c_2=2$ to allow the product $c_1 r_1$ or $c_2 r_2$ to have a mean of 1. The performance of PSO is very sensitive to the inertia weight (ω) parameter which may decrease with the number of iteration as follows (Shi *et al.* 2001)

$$\omega = \omega_{\max} - \frac{\omega_{\max} - \omega_{\min}}{t_{\max}} t \quad (13)$$

where ω_{\max} and ω_{\min} are the maximum and minimum values of ω , respectively; and t_{\max} is the limit numbers of optimization iteration.

He *et al.* (2004) proposed a hybrid of PSO and passive congregation called PSOPC in order to improve the performance of PSO as follows

$$\begin{aligned}\mathbf{V}_i^{t+1} &= \omega^t \mathbf{V}_i^t + c_1 r_1 (\mathbf{pbest}_i^t - \mathbf{X}_i^t) + \\ &c_2 r_2 (\mathbf{gbest}^t - \mathbf{X}_i^t) + c_3 r_3 (\mathbf{R}_i^t - \mathbf{X}_i^t)\end{aligned}\quad (14)$$

where \mathbf{R}_i is a particle selected randomly from the swarm, c_3 is the passive congregation coefficient, and r_3 is a uniform random sequence in the range $(0, 1)$.

6. Real coded genetic algorithm with SBX crossover

Generally, genetic algorithms (GAs) consist of five components as follows (Mitsuo and Runnei 2003):

- A genetic representation of solutions for the problem.
- A operator for creating an initial population of solutions.
- An mechanism for evaluation function rating solution in terms of its fitness.

- A mechanism for selecting parent and genetic operators that alter the genetic composition of children during reproduction.

- The parameters that influence on GAs.

Real coded GA (RCGA) has been introduced as a good method for optimization problems with continues variables. Real number encoding performs better than binary or gray encoding for these problems. In RCGA, the tournament selection is utilized as a selection operator. Simulated Binary Crossover (SBX) and polynomial mutation are also adopted as other operators of RCGA.

6.1 Simulated binary crossover

In SBX crossover operator, two children solutions are created from two parents (Subbaraj *et al.* 2011). For this purpose, first, a random number, $u_i \in [0, 1]$, is chosen, and β_{qi} is calculated as given in the following equation

$$\beta_{qi} = \begin{cases} (2u_i)^{\frac{1}{\eta_c+1}} & u_i \leq 0.5 \\ \left(\frac{1}{2(1-u_i)}\right)^{\frac{1}{\eta_c+1}} & \text{otherwise} \end{cases} \quad (15)$$

where η_c is the crossover index. A spread factor β_{qi} is also defined as the ratio of the absolute difference in offspring values to that of the parents. Then, two children solutions are obtained as follows

$$\begin{aligned}\mathbf{X}_i^{(1,t+1)} &= 0.5 \left[(1 + \beta_{qi}) \mathbf{X}_i^{(1,t)} + (1 - \beta_{qi}) \mathbf{X}_i^{(2,t)} \right] \\ \mathbf{X}_i^{(2,t+1)} &= 0.5 \left[(1 - \beta_{qi}) \mathbf{X}_i^{(1,t)} + (1 + \beta_{qi}) \mathbf{X}_i^{(2,t)} \right]\end{aligned}\quad (16)$$

6.2 Polynomial mutation

Newly generated offspring undergoes polynomial mutation operation. Like in the SBX operator, the probability distribution can also be a polynomial function, instead of a normal distribution. The new offspring $\mathbf{Y}_i^{(1,t+1)}$ is determined as follows (Deb 2001)

$$\mathbf{Y}_i^{(1,t+1)} = \mathbf{X}_i^{(1,t+1)} + (\mathbf{X}_i^U - \mathbf{X}_i^L) \delta_i \quad (17)$$

where \mathbf{X}_i^U and \mathbf{X}_i^L are the upper and lower limit values. The parameter δ_i is obtained from the polynomial probability distribution

$$P(\delta) = 0.5(\eta_m + 1)(1 - |\delta|)^{\eta_m} \quad (18)$$

7. The proposed intelligent ANFIS method

The ANFIS approach utilizes both the advantages of neural networks and fuzzy systems. However, training the parameters of the ANFIS model is considered as a main challenge when ANFIS is employed for the real-world problems. Furthermore, the GD approaches are utilized as the training methods of ANFIS, which are known to be local search approaches and their performances generally

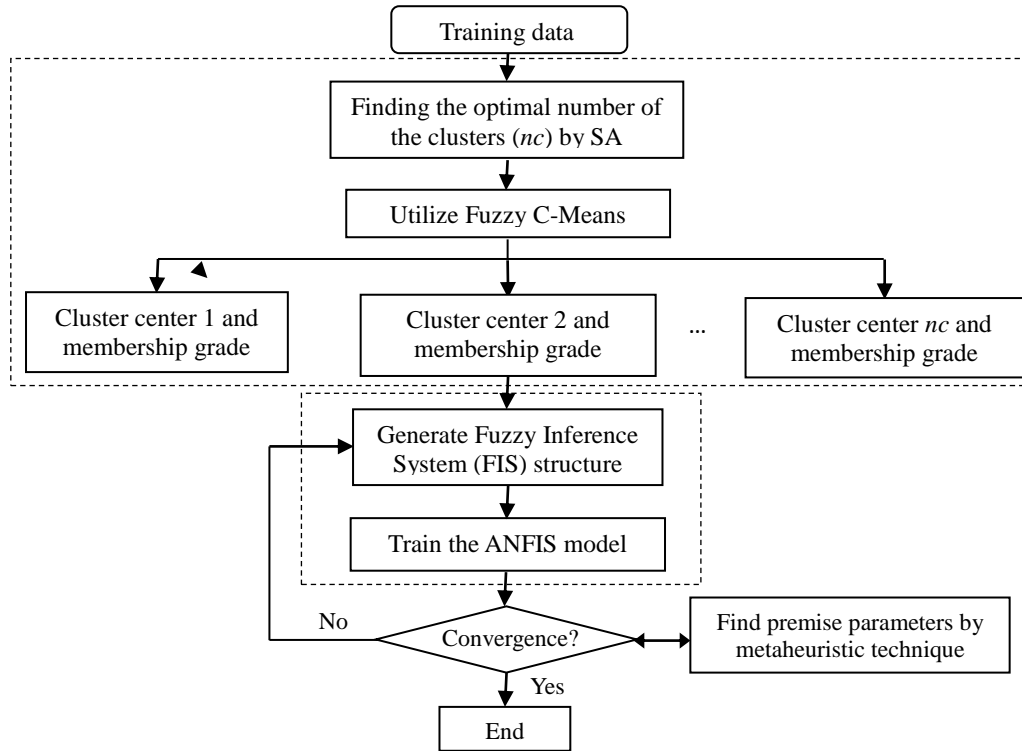


Fig. 3 Flowchart of the proposed intelligent ANFIS method

depend on initial values of parameters. Since the optimal design of fuzzy systems (FSs) can be considered as an optimization problem, many researchers have proposed metaheuristic approaches such as genetic algorithms (Juang 2002, Mansoori *et al.* 2006, Khoshbin *et al.* 2016) and PSO (Araujo *et al.* 2008, El-Zonkoly *et al.* 2009; Das Sharma *et al.* 2009) for the optimal design of FSs.

The performance and accuracy of the ANFIS model depend on the premise parameters and the consequent parameters which need to be trained. In order to improve and increase the accuracy of the ANFIS model in this study, the premise parameters i.e., $\{a_i, b_i, c_i\}$ are estimated by the PSOPC and RCGA methods, which considered as the design variables of optimization problem. Furthermore, the consequent parameters are calculated by the least squares estimation (LSE). To evaluate the accuracy of the PSO-ANFIS and RCGA-ANFIS approaches, the root mean squared error (RMSE) between actual output and desired output is considered as the objective function, which can be expressed as follows

$$RMSE = \sqrt{\frac{\sum_{i=1}^n (y_i - \bar{y}_i)^2}{n}} \quad (19)$$

where y and \bar{y} are the measurement values and the predicted values, respectively; and n is the total number of test data. In fact, RMSE can calculate the variation of errors in the proposed model and is very useful when large errors are undesirable.

In a conventional fuzzy inference system, the number of fuzzy rules is determined by the user's experience who is familiar with the target system to be modeled. In the

simulation of ANFIS, no expert is available and the number of MFs assigned to each input variable is chosen by trial and error. Hence, in the proposed method the subtractive algorithm (SA) (Chiu 1994) is utilized to find the optimum number of the fuzzy rules. The fuzzy c-means (FCM) approach (Bezdek 1981) also creates a fuzzy inference system for the antecedents and consequents. The details of the SA and FCM approaches can be found in the work of Khatibinia *et al.* (2012). The flowchart of the proposed intelligent ANFIS method is shown in Fig. 3.

8. Numerical results

8.1 Scaling and dividing database

To evaluate the effectiveness and accuracy of the proposed approach, the debonding resistance of FRP retrofitted masonry elements is estimated using the PSOPC-ANFIS and RCGA-ANFIS approaches. In order to achieve this purpose, the database of laboratory testing results for 109 samples outlined in Table 1 is selected. In the database, the input variables consist of thickness of the FRP strip (t_p), width of the FRP strip (b_p), Young's modulus of the FRP (E_p), bonded length (L_b), tensile strength of the masonry block (f_{ut}), width of the masonry block (b_m). The maximum debonding force (P_{max}) is also considered as the output variable. Before scaling and dividing database, the values of the input variables are normalized between 0.2 and 0.8 as follows

$$\bar{x}_i = b_1 \frac{x_i - x_{min}}{x_{max} - x_{min}} + b_2 \quad (20)$$

where \bar{x}_i , x_{\max} and x_{\min} are the normalized, maximum and minimum values of the input variables, respectively. In this study, b_1 and b_2 are assumed to be equal to 0.6 and 0.2, respectively. Then, the database is randomly divided into training and testing sets including 87 and 22 samples, respectively.

8.2 The PSOPC and RCGA design

The performance and the accuracy of PSOPC-ANFIS and RCGA-ANFIS depend on the main parameters of PSOPC and RCGA, respectively. These parameters are utilized in the PSOPC and RCGA design. Hence, in this study the values of these parameters are determined using a trial and error procedure as given in Tables 2 and 3.

Table 2 Parameters of the PSOPC algorithm

Parameters	Value
Number of particles	25
Number of iterations	1000
Passive congregation coefficient	0.5
Initial inertia weight	0.4
Final inertia weight	0.9

Table 3 Parameters of the RCGA algorithm

Parameters	Value
Population Size	25
Number of iterations	1000
Crossover percentage	0.8
Mutation percentage	0.3
Crossover index	5
Mutation index	20

8.3 Estimating accuracy evaluation

To explore and evaluate the accuracy of the proposed PSOPC-ANFIS and RCGA-ANFIS in estimating the debonding strength, different statistical criterions are utilized. The accuracy is computed as a function of the debonding strength. Mean Absolute Error (*MAE*), Mean Absolute Percentage Error (*MAPE*) and Coefficient of Determination (R^2) are considered as the statistical criteria. The *MAE* is a quantity adopted to measure how closely a prediction matches the outcome. The *MAE* is expressed as follows

$$MAE = \frac{1}{n} \sum_{i=1}^n |y_i - \bar{y}_i| \tag{21}$$

Small denominators are problematic for the *MAPE* because they generate higher *MAPE* values impacting the overall value. The *MAPE* is given as follows

$$MAPE = \frac{1}{n} \sum_{i=1}^n \frac{|y_i - \bar{y}_i|}{y_i} \times 100 \tag{21}$$

The R^2 represents the degree to which two variables are linearly related and is expressed as

$$R^2 = \frac{\left(\sum_{i=1}^n (y_i - y_{ave})(\bar{y}_i - \bar{y}_{ave}) \right)^2}{\sum_{i=1}^n (y_i - y_{ave})^2 \sum_{i=1}^n (\bar{y}_i - \bar{y}_{ave})^2} \tag{21}$$

where y_{ave} and \bar{y}_{ave} are the mean of the measurement and predicted values in the data samples.

According to the statistical criteria, the statistic results from PSOPC-ANFIS and RCGA-ANFIS are summarized in Table 4 for the training and testing processes.

Table 4 indicates that, as compared with the RCGA-ANFIS model, the PSOPC-ANFIS model shows the best performance with the highest R^2 . Furthermore, Table 4 reveals the direct relationship between R^2 and the *MAE* and *MAPE* criteria. The performance and the accuracy of the PSOPC-ANFIS and RCGA-ANFIS models are graphically shown in Figs. 4 through 7.

Table 4 The statistical results of the PSOPC-ANFIS and RCGA-ANFIS models

Model	Training process			Testing process		
	<i>MAE</i>	<i>MAPE</i>	R^2	<i>MAE</i>	<i>MAPE</i>	R^2
PSOPC-ANFIS	1.1623	10.1540	0.9947	1.5573	12.5809	0.9915
RCGA-ANFIS	1.5305	11.517	0.9895	2.3818	14.2869	0.9882

It is observed from Figs. 4 through 7, the PSOPC-ANFIS model in comparison with the RCGA-ANFIS model predicts the debonding strength at high accuracy rate. Figs. 4(c) to 7(c) show the distribution of error values from the prediction using the PSOPC-ANFIS and RCGA-ANFIS models. The histograms represented by the models are close to the normal distribution, which illuminate the robust prediction using these models.

Fig. 8 shows the scatter diagrams for the actual values and the predicted values of the testing data of the PSOPC-ANFIS and RCGA-ANFIS models, respectively. As obvious from the figure, the debonding strength estimates of the models are closer to the corresponding measured values although the PSOPC-ANFIS model performs better than the RCGA-ANFIS model.

Using the simulated results of PSOPC-ANFIS and RCGA-ANFIS, the worst, mean, average, best and standard deviation are evaluated from the twenty simulated runs with the computational times given in Table 5.

Table 5 Statistical results of 20 independent runs for the proposed models

Method	Worst	Best	Mean	Standard deviation
PSO-ANFIS	2.357	1.714	2.103	0.6188
RCGA-ANFIS	3.865	2.234	3.169	1.0151

The standard deviation of the results of PSOPC-ANFIS in the twenty independent runs is smaller than that of RCGA-ANFIS. Thus, the PSOPC-ANFIS model is more stable. Also, the convergence curves of both PSOPC-

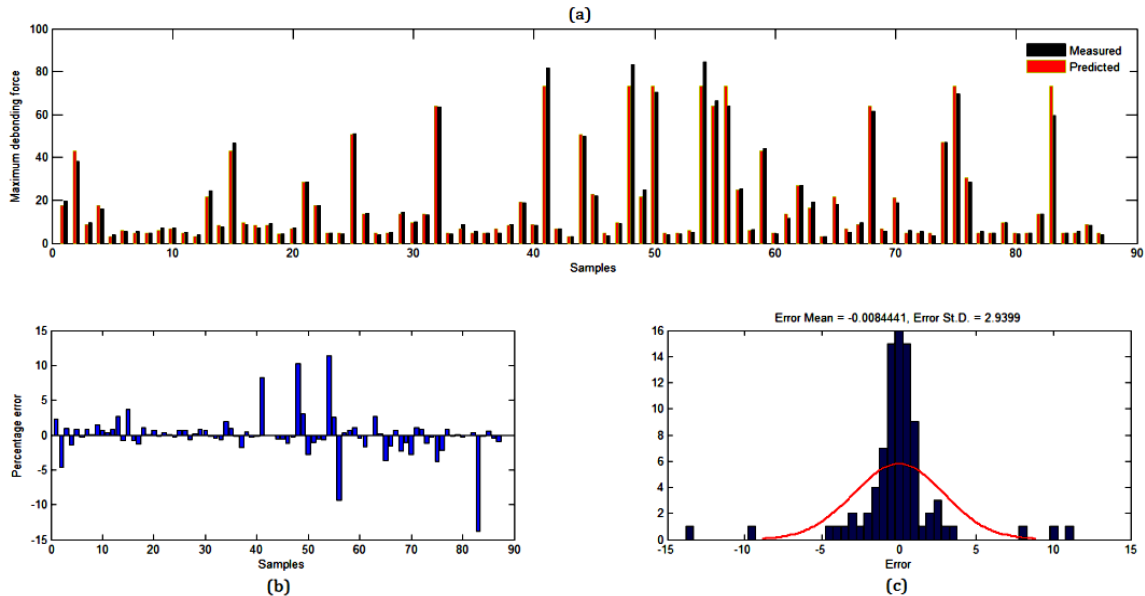


Fig. 4 Results of PSOPC-ANFIS in the training process: (a)Comparison between the measurement and predicted debonding strength, (b)Error value between the measurement and predicted debonding strength and (c)The histogram for distribution of error values

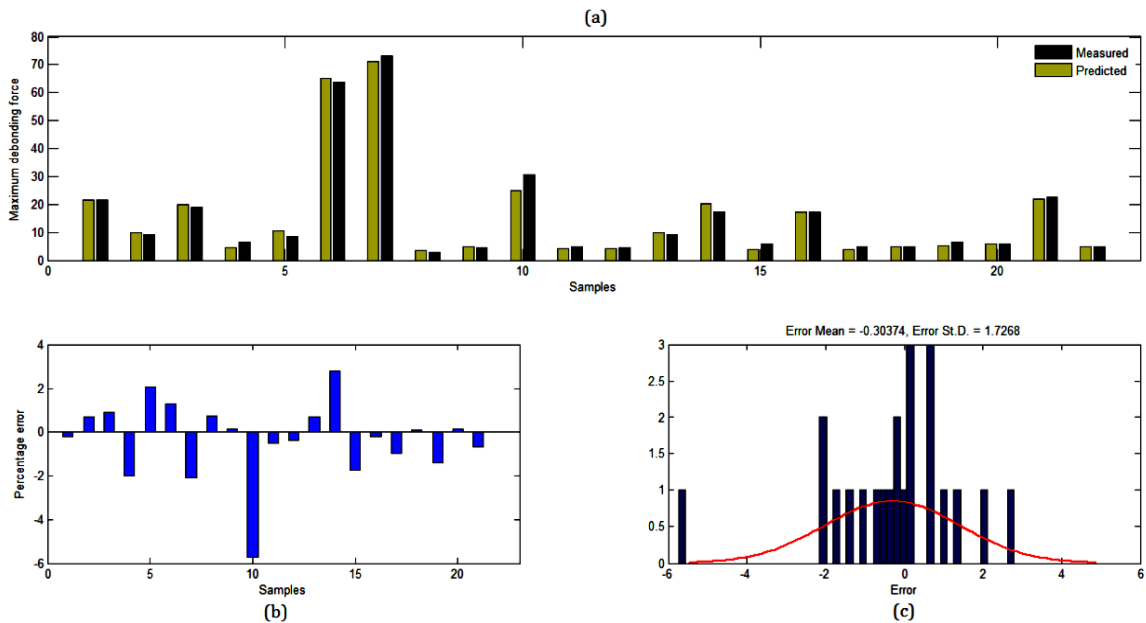


Fig. 5 Results of PSOPC-ANFIS in the testing process: (a)Comparison between the measurement and predicted debonding strength, (b)Error value between the measurement and predicted debonding strength and (c)The histogram for distribution of error values

ANFIS and RCGA-ANFIS are depicted in Fig. 9. As can be seen in Fig. 9, the PSOPC-ANFIS obtains the best solution at 684 iterations. Meanwhile, the RCGA-ANFIS requires 804 iterations. Therefore, the convergence rate of the PSOPC-ANFIS is faster than that of the RCGA-ANFIS.

8.4 Comparison of results with other techniques

This section presents the comparison of PSOPC-ANFIS and RCGA-ANFIS with other prediction techniques including the original ANFIS, ANN and MNLN approaches.

The results of the PSOPC-ANFIS and RCGA-ANFIS models were obtained as explained in the previous section. In order to clarify an overall comparison, all statistical criteria used in training and testing data are combined to create a normalized reference index (*RI*) as follows (Chou *et al.* 2011)

$$RI = \frac{RMSE + MAPE}{2} \quad (24)$$

Table 6 shows the results from the proposed methods, the original ANFIS, ANN and MNLN techniques for

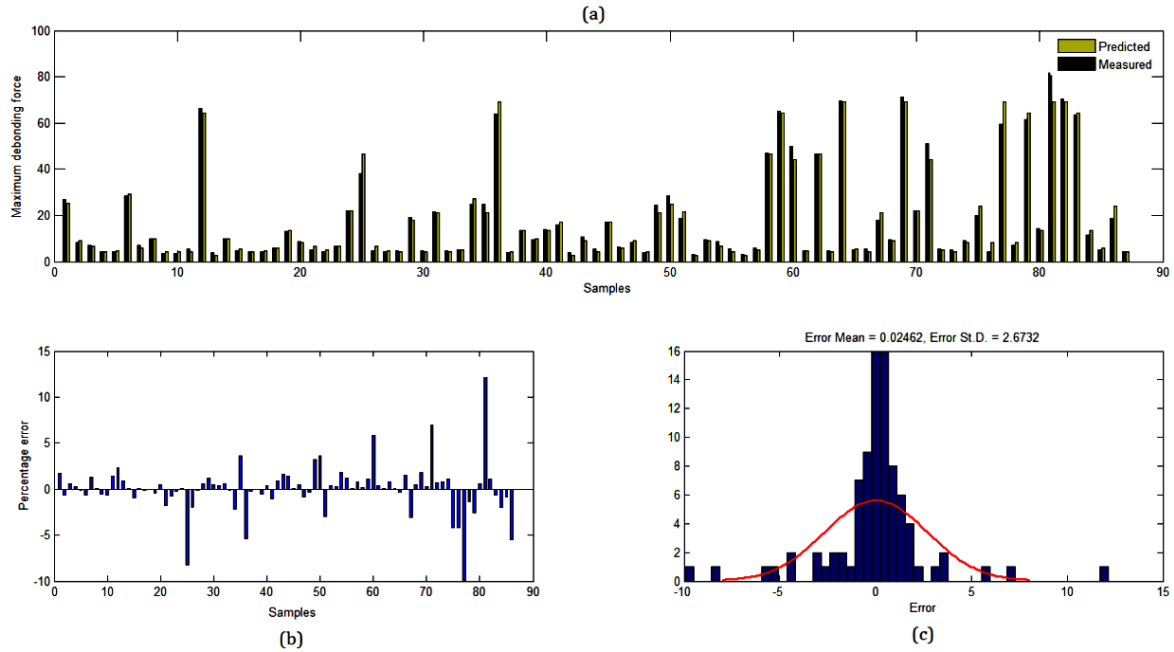


Fig. 6 Results of RCGA-ANFIS in the training process: (a) Comparison between the measurement and predicted debonding strength, (b) Error value between the measurement and predicted debonding strength and (c) The histogram for distribution of error values

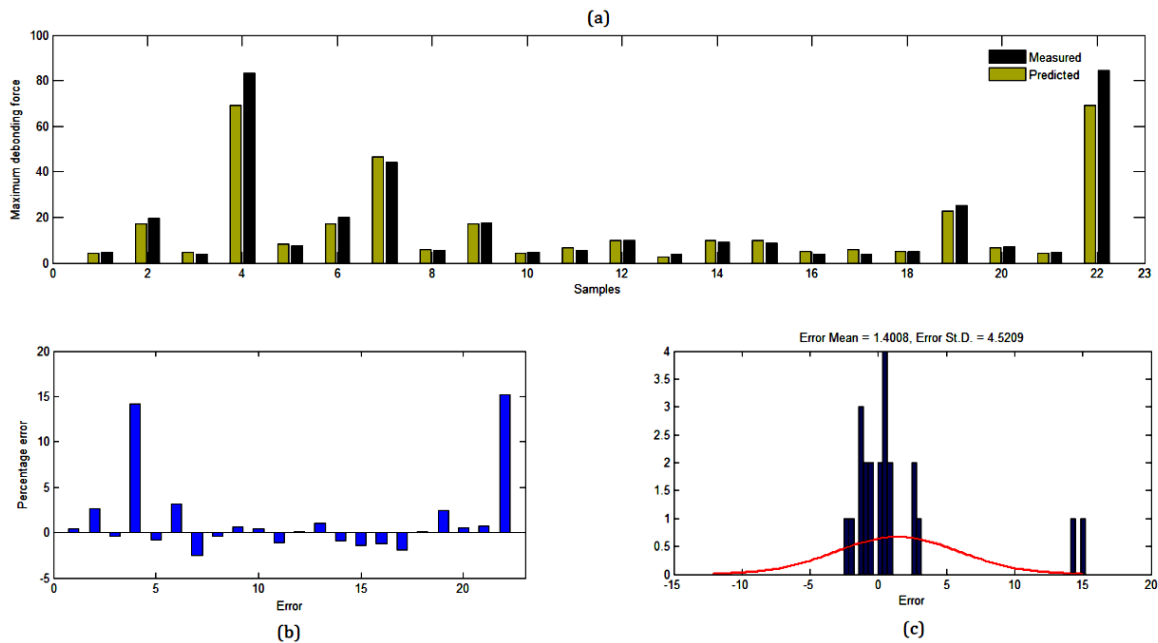


Fig. 7 Results of RCGA-ANFIS in the testing process: (a) Comparison between the measurement and predicted debonding strength, (b) Error value between the measurement and predicted debonding strength and (c) The histogram for distribution of error values

comparison purposes. Based on the *RI* index obtained for testing process, the proposed methods outperform the other techniques. It can also be observed from Table 6 that the PSOPC-ANFIS model is a powerful technique with high accuracy as compared with the other techniques.

Furthermore, the comparison of the PSOPC-ANFIS, RCGA-ANFIS, ANN, ANFIS, MNL and existing bond strength models is established for 109 experimental data in Table 7. The mean, median, maximum, minimum and

standard division (SD) statistics for each model are normalized based on the suggestion proposed by Mansouri and Kisi (2015). A value close to 1 for these criteria demonstrates desirable accuracy. It is obvious from Table 8 that the criterions obtained by the PSOPC-ANFIS and RCGA-ANFIS models are closer to the measured values. Thus, the proposed models are reliably utilized for modeling debonding strength of masonry elements retrofitted with FRP.

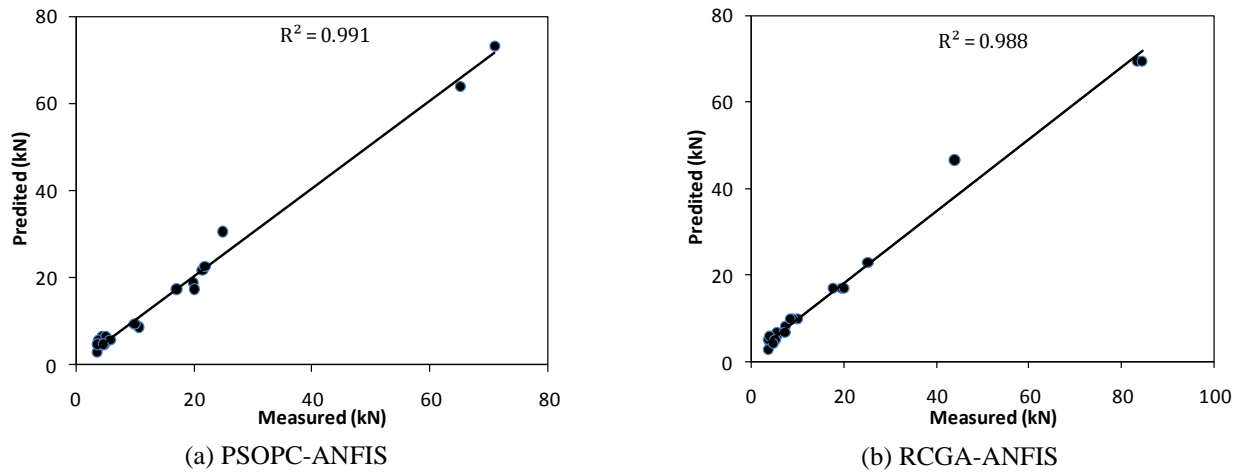


Fig. 8 The scatter plots of the measured and estimated debonding strength values in the testing process

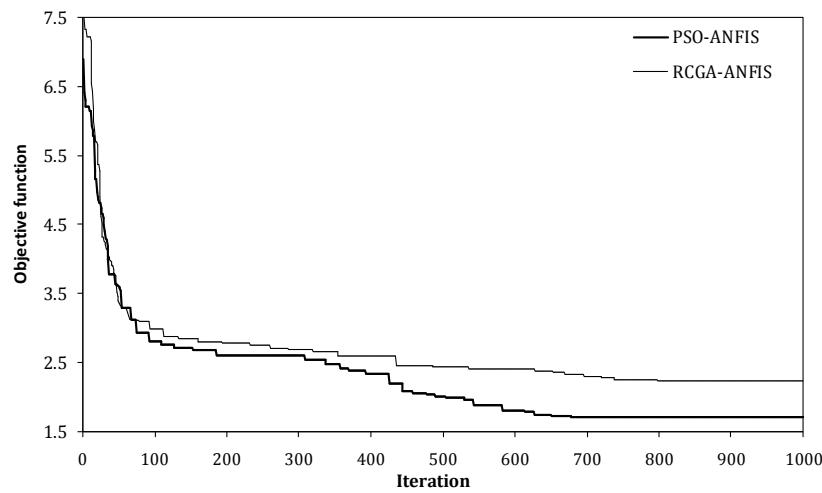


Fig. 9 Convergence curves of the best results for the RCGA-ANFIS and PSOPC-ANFIS

Table 6 Performance measurement results of various prediction techniques

Model	Training process			Testing process			
	MAPE	RMSE	R^2	MAPE	RMSE	RI	R^2
PSOPC-ANFIS	10.154	2.2930	0.9947	12.5809	1.7142	1.0	0.9915
RCGA-ANFIS	11.517	2.6579	0.9895	14.2869	2.2338	0.7621	0.9882
Original ANFIS	8.24	2.784	0.984	16.6	2.771	0.4787	0.977
ANN	7.85	2.773	0.984	14.9	2.423	0.6761	0.981
MNLR	12.5	4.121	0.967	19.9	3.856	0.0	0.950

 Table 7 Statistical results of P_{max} for ANN, ANFIS, MNLR and the proposed models

Model	Mean	Median	Max	Min	SD
Measured	17,155	8470	70,360	2850	17,623
ANN	1.013	1.025	1.042	1.292	1.024
ANFIS	0.976	1.017	1.042	1.355	1.016
MNLR	0.997	0.982	0.934	1.105	0.97
PSOPC-ANFIS	1.073	0.971	1.040	1.027	1.195
RCGA-ANFIS	1.052	0.977	0.986	0.975	1.152

9. Conclusions

This study develops intelligent the ANFIS approach to model debonding strength of masonry elements retrofitted with FRP. In the proposed approach, the PSOPC and RCGA are employed to find the optimal parameters for membership functions and fuzzy rules in ANFIS which can generate a model for the debonding strength with high accuracy. The comparison of results from the proposed PSOPC-ANFIS and the RCGA-ANFIS indicates that the PSOPC-ANFIS model is significantly more accurate than

the RCGA-ANFIS model. Also, PSOPC-ANFIS outperforms RCGA-ANFIS in terms of coverage rate due to the stronger global search ability of the PSOPC algorithm. Finally, from the validation test results, it can be found that the modeling accuracy based on the proposed approach is significantly higher than the one based on the ANN, ANFIS and MNLN approaches in terms of Mean Absolute Percentage Error (MAPE), Coefficient of Determination (R^2), and the normalized reference index (RI). Hence, the presented results validate the proficiency of the proposed approach in debonding strength prediction. Therefore, the proposed PSOPC-ANFIS method had better performance than the RCGA-ANFIS model and the conventional ANFIS trained with the gradient decent method due to the stronger global search ability of the PSOPC algorithm. Although the computational cost of the PSOPC-ANFIS method is higher than that for the conventional ANFIS. In future research, another optimization techniques may be developed to replace the PSOPC and RCGA techniques used in this study for further comparison.

References

- Abdollahi Chahkand, N., Zamin Jumaat, M., Ramli Sulong, N.H., Zhao, X.L. and Mohammadzadeh, M.R. (2014), "Experimental and theoretical investigation on torsional behavior of CFRP strengthened square hollow steel section", *Thin. Wall. Struct.*, **68**, 135-140.
- Alshihri, M.M., Azmy, A.M. and El-Bisy, M.S. (2009), "Neural networks for predicting compressive strength of structural light weight concrete", *Constr. Build. Mater.*, **23**, 2214-2219.
- Araujo, E. and Coelho, L.D.S. (2008), "Particle swarm approaches using Lozi map chaotic sequences to fuzzy modeling of an experimental thermal-vacuum system", *App. Soft. Comput.*, **8**, 1354-1364.
- Atici, U. (2011), "Prediction of the strength of mineral admixture concrete using multivariable regression analysis and an artificial neural network", *Exp. Syst. Appl.*, **38**, 9609-9618.
- Bal, L. and Buyle-Bodin, F. (2013), "Artificial neural network for predicting drying shrinkage of concrete", *Constr. Build. Mater.*, **38**, 248-254.
- Bedirhanoglu, I. (2014), "A practical neuro-fuzzy model for estimating modulus of elasticity of concrete", *Struct. Eng. Mech.*, **51**(2), 249-265.
- Bezdek, J.C. (1981), *Pattern Recognition with Fuzzy Objective Function Algorithms*, Plenum Press, New York.
- Carrara, P. and Freddi, F. (2014), "Statistical assessment of a design formula for the debonding resistance of FRP reinforcements externally glued on masonry units", *Compos. Part B. Eng.*, **66**, 65-82.
- Ceroni, F., Ferracuti, B., Pecce, M. and Savoia, M. (2014), "Assessment of a bond strength model for FRP reinforcement externally bonded over masonry blocks", *Compos. Part B. Eng.*, **61**, 147-161.
- Ceroni, F., Garofano, F. and Pecce, M. (2014), "Modeling of the bond behavior of tuff elements externally bonded with FRP sheets", *Compos. Part B. Eng.*, **59**, 248-259.
- Chen, J.F. and Teng, J.G. (2001), "Anchorage strength models for FRP and steel plates bonded to concrete", *J. Struct. Eng.*, ASCE, **127**, 784-791.
- Chitti, H., Khatibinia, M., Akbarpour, A. and Naseri, H.R. (2016), "Reliability-based design optimization of concrete gravity dams using subset simulation", *Int. J. Optim. Civil. Eng.*, **6**(3), 329-348.
- Chou, J.S., Chiu, C.K., Farfoura, M. and Al-Taharwa, I. (2011), "Optimizing the prediction accuracy of concrete compressive strength based on a comparison of data-mining techniques", *J. Comput. Civ. Eng.*, **25**, 242-253.
- D'Antino, T. and Pellegrino, C. (2014), "Bond between FRP composites and concrete: assessment of design procedures and analytical models", *Compos. Part B. Eng.*, **60**, 440-456.
- Das Sharma, K., Chatterjee, A. and Rakshit, A. (2009), "A hybrid approach for design of stable adaptive fuzzy controllers employing Lyapunov theory and particle swarm optimization", *IEEE. T. Fuzzy. Syst.*, **17**, 329-342.
- De Lorenzis, L., Paggi, M., Carpinteri, A. and Zavarise, G. (2010), "Linear elastic fracture mechanics approach to plate end debonding in rectilinear and curved plated beams", *Int. J. Sol. Struct.*, **13**, 875-889.
- Deb, K. (2001), *Multi Objective Optimization using Evolutionary Algorithms*, John Wiley & Sons.
- El-Zonkoly, A.M., Khalil, A.A. and Ahmied, N.M. (2009), "Optimal tuning of lead-lag and fuzzy logic power system stabilizers using particle swarm optimization", *Expert. Syst. Appl.*, **36**, 2097-2106.
- Ferracuti, B., Savoia, M. and Mazzotti, C. (2006), "A numerical model for FRP concrete delamination", *Compos. Part B. Eng.*, **37**, 356-364.
- Ferracuti, B., Savoia, M. and Mazzotti, C. (2007), "Interface law for FRP-concrete delamination", *Compos. Struct.*, **80**, 523-531.
- Gharehbaghi, S. and Khatibinia, M. (2015), "Optimal seismic design of reinforced concrete structures under time history earthquake loads using an intelligent hybrid algorithm", *Earthq. Eng. Vib.*, **14**, 97-109.
- Gholizadeh, S. (2015), "Performance-based optimum seismic design of steel structures by a modified firefly algorithm and a new neural network", *Adv. Eng. Soft.*, **81**, 50-65.
- Gholizadeh, S. and Salajegheh, E. (2009), "Optimal design of structures for time history loading by swarm intelligence and an advanced metamodel", *Comput. Method. Appl. Eng.*, **198**, 2936-2949.
- Gholizadeh, S., Salajegheh, J. and Salajegheh, E. (2009), "An intelligent neural system for predicting structural response subject to earthquakes", *Adv. Eng. Soft.*, **40**, 630-639.
- Golafshani, E.M., Rahai, A., Sebt, M.H. and Akbarpour, H. (2012), "Prediction of bond strength of spliced steel bars in concrete using artificial neural network and fuzzy logic", *Constr. Build. Mater.*, **36**, 411-418.
- He, S., Wu, Q.H., Wen, J.Y., Saunders, J.R. and Paton, R.C. (2004), "A particle swarm optimizer with passive congregation", *Biosystems.*, **78**, 135-147.
- Helmy, T., Rasheed, Z. and Al-Mulhem, M. (2011), "Adaptive fuzzy logic-based framework for handling imprecision and uncertainty in classification of bioinformatics datasets", *Int. J. Comput. Meth.*, **8**, 513-534.
- Jalal, M. and Ramezaniapour, A.A. (2012), "Strength enhancement modeling of concrete cylinders confined with CFRP composites using artificial neural networks", *Compos. Part B. Eng.*, **43**, 2990-3000.
- Jang, J.S.R., Sun, C.T. and Mizulani, E. (1996), *Neuro-fuzzy and Soft Computing: a Computational Approach to Learning and Machine Intelligence*, Prentice-Hall.
- Juang, C.F. (2002), "A TSK-type recurrent fuzzy network for dynamic systems processing by neural network and genetic algorithms", *IEEE. T. Fuzzy. Syst.*, **10**, 155-170.
- Kashyap, J., Willis, C.R., Griffith, M.C., Ingham, J.M. and Masia, M.J. (2012), "Debonding resistance of FRP-to-clay brick masonry joints", *Eng. Struct.*, **41**, 186-198.
- Kennedy, J., Eberhart, R.C. and Shi, Y. (2001), *Swarm Intelligence*, Morgan Kaufman Publishers.
- Khalifa, A., Gold, W., Nanni, A. and Abdel Aziz, M.I. (1998),

- “Contribution of externally bonded FRP to shear capacity of RC flexural members”, *J. Compos. Constr.*, **2**, 195-202.
- Khatibinia, M. and Khosravi, Sh. (2014), “A hybrid approach based on an improved gravitational search algorithm and orthogonal crossover for optimal shape design of concrete gravity dams”, *Appl. Soft. Comput.*, **16**, 223-233.
- Khatibinia, M., Chitti, H., Akbarpour, A. and Naseri, H.R. (2016), “CShape optimization of concrete gravity dams considering dam-water-foundation interaction and nonlinear effects”, *Int. J. Optim. Civil Eng.*, **6**(1), 115-34.
- Khatibinia, M., Fadaee, M.J., Salajegheh, J. and Salajegheh, E. (2013), “Seismic reliability assessment of RC structures including soil-structure interaction using wavelet weighted least squares support vector machine”, *Reliab. Eng. Syst. Saf.*, **110**, 22-33.
- Khatibinia, M., Gharehbagh, S. and Moustafa, A. (2015), “Seismic reliability-based design optimization of reinforced concrete structures including soil-structure interaction effects”, *Earthquake Engineering-From Engineering Seismology to Optimal Seismic Design of Engineering Structure*, 267-304.
- Khatibinia, M., Salajegheh, E., Salajegheh, J. and Fadaee, M.J. (2013), “Reliability-based design optimization of RC structures including soil-structure interaction using a discrete gravitational search algorithm and a proposed metamodel”, *Eng. Optim.*, **45**, 1147-1165.
- Khatibinia, M., Salajegheh, J., Fadaee, M.J. and Salajegheh, E. (2012), “Prediction of failure probability for soil-structure interaction system using modified ANFIS by hybrid of FCM-FPSO”, *Asian. J. Civil. Eng.*, **13**, 1-27.
- Khoshbin, F., Bonakdari, H., Ashraf Talesh, S.H., Ebtehaj, I., Zaji, A.H. and Azimi, H. (2016), “Adaptive neuro-fuzzy inference system multi-objective optimization using the genetic algorithm/singular value decomposition method for modeling the discharge coefficient in rectangular sharp-crested side weirs”, *Eng. Optim.*, **48**, 933-948.
- Mansoori, E.G., Zolghadri, M.J. and Katebi, S.D. (2008), “SGERD: a steady-state genetic algorithm for extracting fuzzy classification rules from data”, *IEEE. T. Fuzzy. Syst.*, **16**(4), 1061-1071.
- Mansouri, I. and Kisi, O. (2015), “Prediction of debonding strength for masonry elements retrofitted with FRP composites using neuro fuzzy and neural network approaches”, *Compos. Part B. Eng.*, **70**, 247-255.
- Mitsuo, G. and Runnei, C. (2000), *Genetic Algorithms and Engineering Optimization*, John Wiley & Sons Inc.
- Mohammadzadeh, M.R. and Fadaee, M.J. (2009), “Torsional behavior of high-strength concrete beams strengthened using CFRP sheets; an experimental and analytical study”, *Int. J. Sci. Technol.*, **16**, 321-330.
- Mohammadzadeh, M.R. and Fadaee, M.J. (2010), “Experimental and analytical Study on behavior of CFRP strengthened HSC beams with minimum torsional reinforcement”, *Iran. J. Sci. Technol.*, **34**, 35-48.
- Mohammadzadeh, M.R., Fadaee, M.J. and Ronagh, H.R. (2009), “Improving torsional behavior of reinforced concrete beams strengthened with carbon fiber reinforced polymer composite”, *Iran. Polym. J.*, **18**, 315-327.
- Oliveira, D.V., Basilio, I. and Lourenco, P.B. (2010), “Experimental bond behavior of FRP sheets glued on brick masonry”, *J. Compos. Constr.*, **15**, 32-41.
- Ozcan, F., Atis, C.D., Karahan, O., Uncuoglu, E. and Tanyildizi, H. (2009), “Comparison of artificial neural network and fuzzy logic models for prediction of long-term compressive strength of silica fume concrete”, *Adv. Eng. Soft.*, **40**, 856-863.
- Pan, J. and Leung, C.K.Y. (2007), “Debonding along the FRP-concrete interface under combined pulling/peeling effects”, *Eng. Fract. Mech.*, **74**, 132-150.
- Perera, R., Tarazona, D., Ruiz, A. and Martin, A. (2014), “Application of artificial intelligence techniques to predict the performance of RC beams shear strengthened with NSM FRP rods. Formulation of design equations”, *Compos. Part B. Eng.*, **66**, 162-173.
- Plevris, V. and Asteris, P.G. (2014), “Modeling of masonry failure surface under biaxial compressive stress using Neural Networks”, *Constr. Build. Mater.*, **55**, 447-461.
- Sadrmomtazi, A., Sobhani, J. and Mirgozar, M.A. (2013), “Modeling compressive strength of EPS lightweight concrete using regression, neural network and ANFIS”, *Constr. Build. Mater.*, **42**, 205-216.
- Sayed-Ahmed, E.Y., Bakay, R. and Shrive, N.G. (2009), “Bond strength of FRP laminates to concrete: state-of-the-art review”, *J. Struct. Eng.*, **9**, 45-61.
- Seyedpoor, S.M., Salajegheh, J., Salajegheh, E. and Gholizadeh, S. (2009), “Optimum shape design of arch dams for earthquake loading using a fuzzy inference system and wavelet neural networks”, *Eng. Optim.*, **41**, 473-493.
- Shi, Y. and Eberhart, R. (1998). “A modified particle swarm optimizer”, *IEEE World Congress on Computational Intelligence, Evolutionary Computation Proceedings*, Anchorage, AK.
- Shi, Y., Liu, H., Gao, L. and Zhang, G. (2011), “Cellular particle swarm optimization”, *Inform. Sci.*, **181**, 4460-4493.
- Slonski, M. (2010), “A comparison of model selection methods for compressive strength prediction of high-performance concrete using neural networks”, *Comput. Struct.*, **88**, 1248-1253.
- Sobhani, J., Najimi, M., Pourkhorshidi, A.R. and Parhizkar, T. (2010), “Prediction of the compressive strength of no-slump concrete: a comparative study of regression, neural network and ANFIS models”, *Constr. Build. Mater.*, **24**, 709-718.
- Subbaraj, P., Rengaraj, R. and Salivahanan, S. (2011), “Enhancement of self-adaptive real-coded genetic algorithm using taguchi method for economic dispatch problem”, *Appl. Soft. Comput.*, **11**, 83-92.
- Tsai, P.W., Hayat, T., Ahmad, B. and Chen, Ch.W. (2015), “Structural system simulation and control via NN based fuzzy model”, *Struc. Eng. Mech.*, **56**(3), 385-407.
- Willis, C.R., Yang, Q., Seracino, R. and Griffith, M.C. (2009), “Bond behavior of FRP-to-clay brick masonry joints”, *Eng. Struct.*, **31**, 2580-2587.
- Yuksel, S.B. and Yazar, A. (2015), “Neuro-fuzzy and artificial neural networks modeling of uniform temperature effects of symmetric parabolic haunched beams”, *Struc. Eng. Mech.*, **56**(5), 787-796.

CC